Electronic Supplementary Material (ESI) for Journal of Materials Chemistry A.

Supporting information

Degradation Mechanism of Planar-Perovskite Solar Cells: Correlating Evolution of Iodine Distribution and Photocurrent Hysteresis

Riski Titian Ginting,[a] Mi-Kyoung Jeon,[a] Won-Yong Jin,[a] Kwang-Jae Lee,[a] Tae-Wook Kim [b, *] and Jae-Wook Kang[a, *]

[a]Department of Flexible and Printable Electronics, Polymer Materials Fusion Research Center, Chonbuk National University, Jeonju 54896, Republic of Korea

*E-mail: jwkang@jbnu.ac.kr

[b]Soft Innovative Materials Research Center, Institute of Advanced Composite Materials, Korea Institute of Science and Technology, Jeollabuk-do 55324, Republic of Korea

*E-mail: twkim@kist.re.kr (T.-W. Kim)

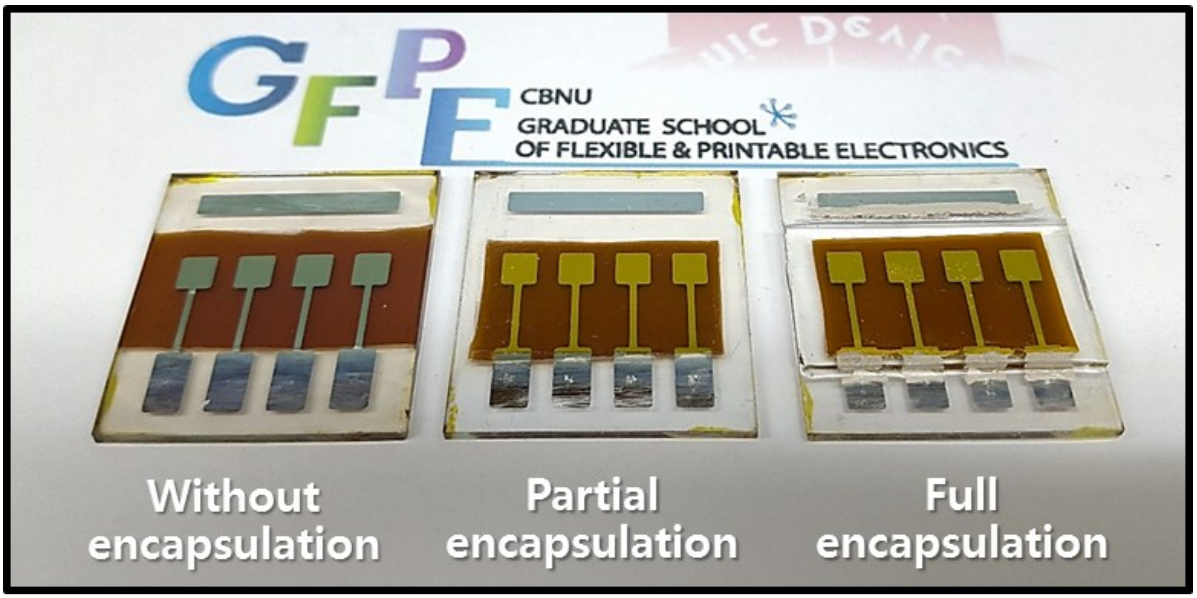

Figure S1. Photography images of PSC devices.

Stability performance analysis

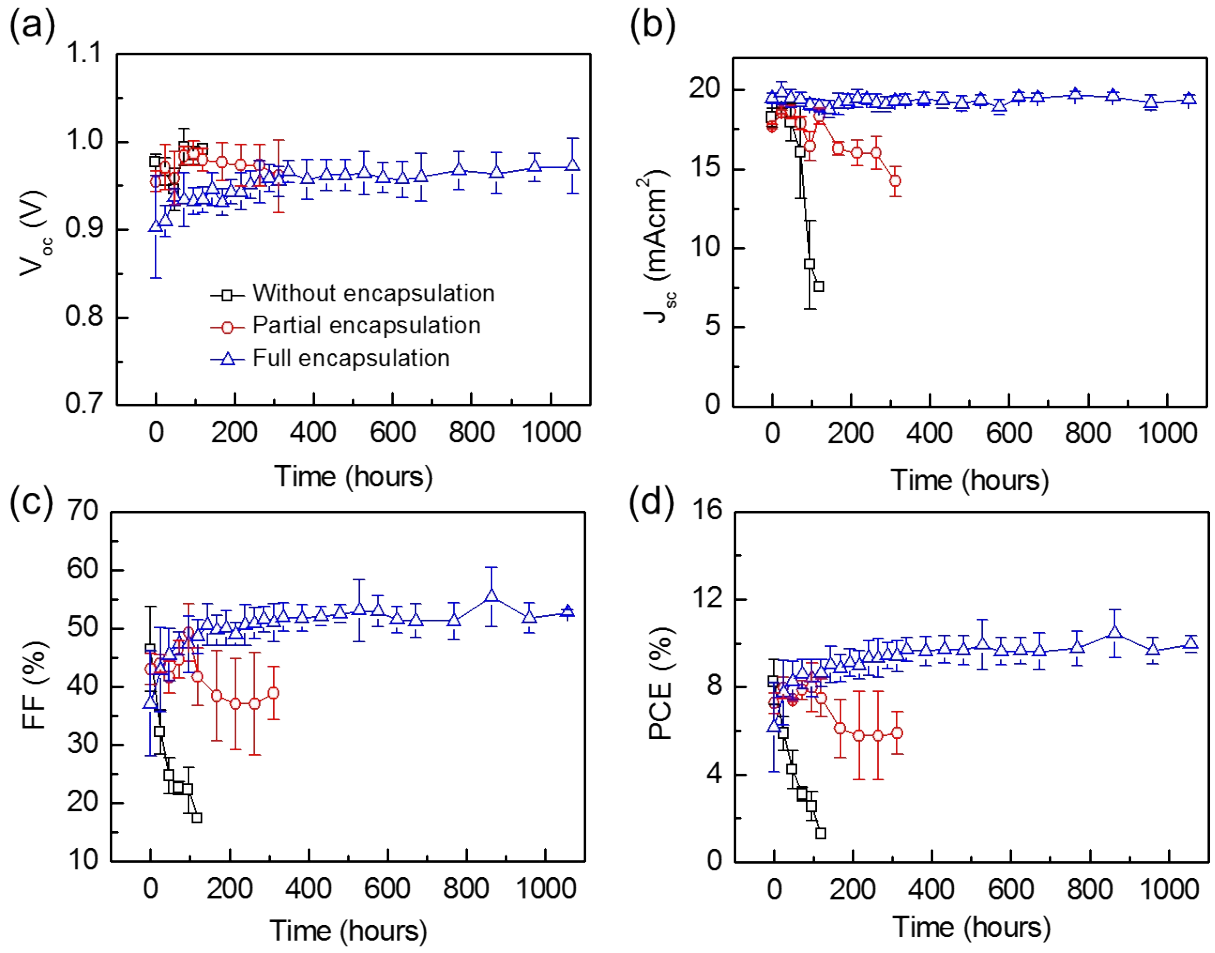

Figure S2. Device performance parameters (a) V_{oc}, (b) J_{sc}, (c) FF, and (d) PCE extracted from *J*–*V* curves as a function of storage time for non-, partial, and fully encapsulated PSC devices measured in the forward scan direction.

Photo-CELIV analysis

The charge carrier mobility and transit time was measured by using the equation reported previously.[1]

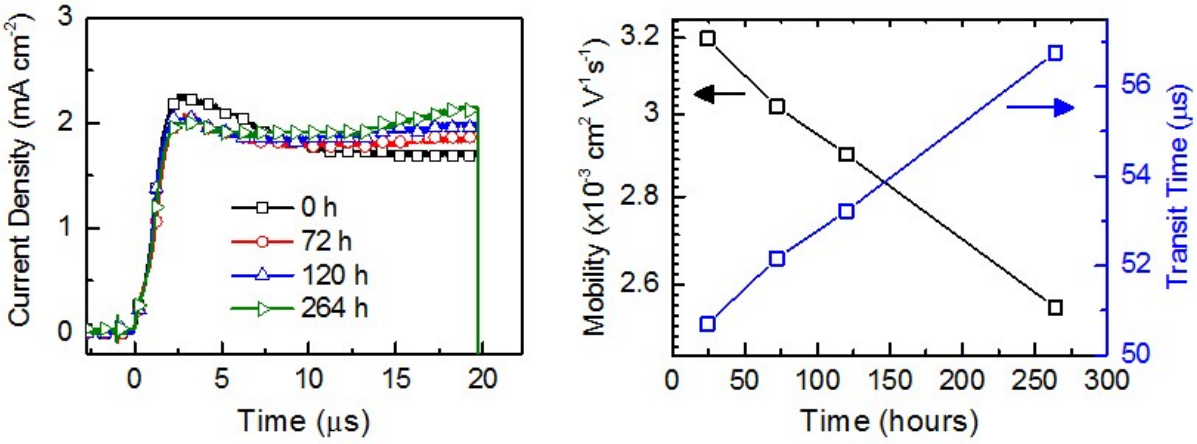

Figure S3. a) Photo-CELIV curves of partially encapsulated PSCs, b) extracted carrier mobility and transient time as function of storage time in dark ambient conditions.

XPS depth profile analysis

Fig. S4a and b shows the XPS depth profile analysis for sample aging after 72 and 240 h in ambient air. Fig. S4c depicts the deconvoluted narrow scan C1s peak for sputter time of 600 s centered at 284.92 and 285.81 eV represents the C-H and C-C component, respectively can be assigned for spiro-OMeTAD layer.[2] Meanwhile, at sputter time of 2000 s the C1s peak shifted to lower binding energy of 284.45 and 285.32 eV which corresponded to the $MAPbI_3$. In order to observe the shifts of iodine element in Fig. 3b, the sputter time of aging sample was all normalized to the initial fresh sample of maximum Pb at% intensity.

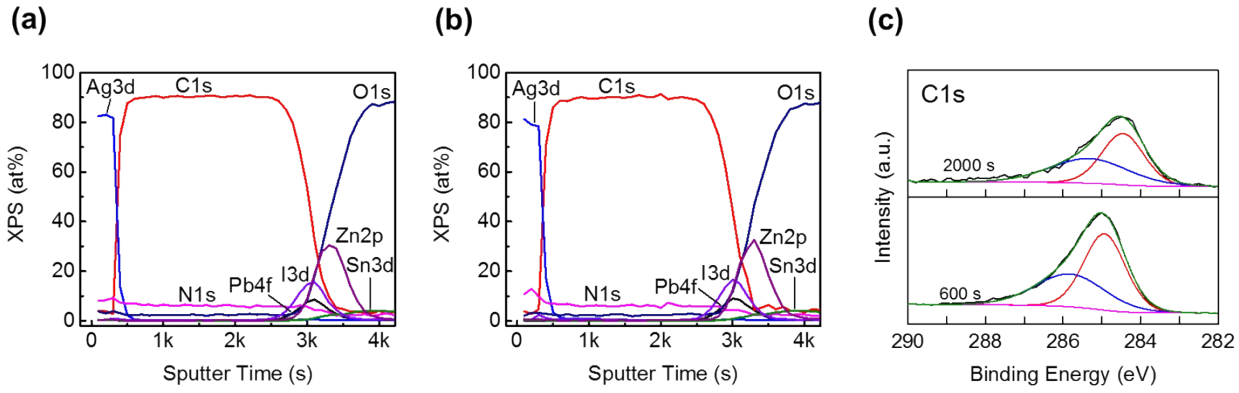

Figure S4. XPS depth profile analysis for device configuration of Ag/spiro-OMeTAD/$MAPbI_3$/ZnO/ITO after aging in ambient air for (a) 72 h and (b) 240 h. (c) Narrow scan of C1s for different sputter time.

Impedance analysis

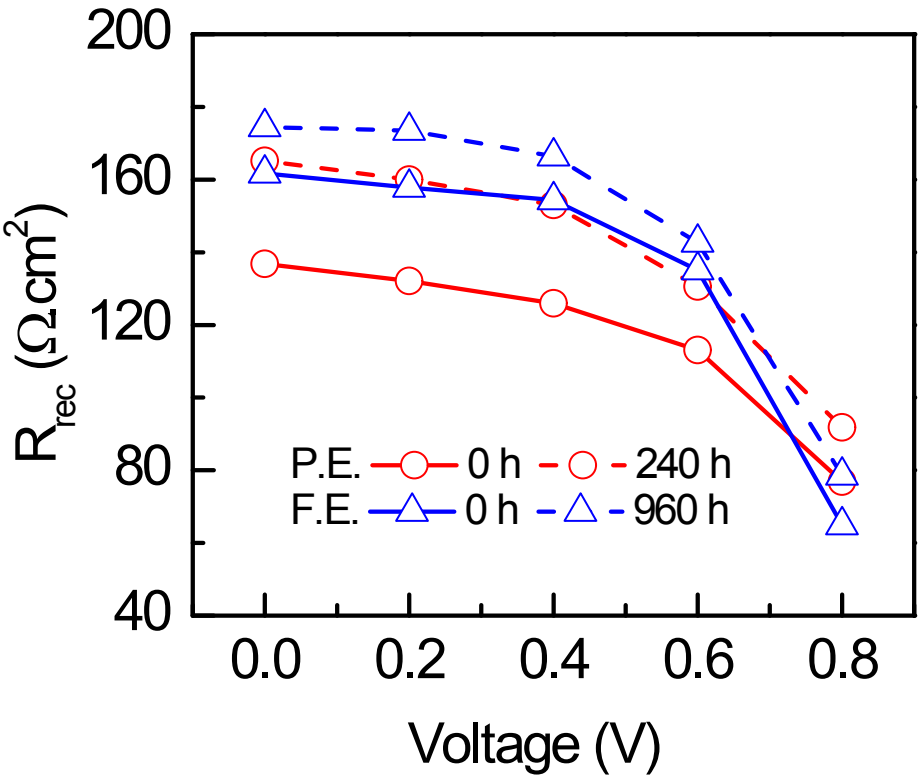

Figure S5. Extracted R_{rec} values as function of applied voltage with 0 and 240 h aged device under white LED illumination.

Hysteresis analysis

Degree of hysteresis (DoH) of PSCs device with different storage time was calculated based on the following equation[3]:

$$DoH = \frac{J_{RS}(0.6V_{oc}) - J_{FS}(0.6V_{oc})}{J_{RS}(0.6V_{oc})} \quad \text{(Eq. S1)}$$

where FS and RS represents the forward and reversed scan voltage direction, respectively.

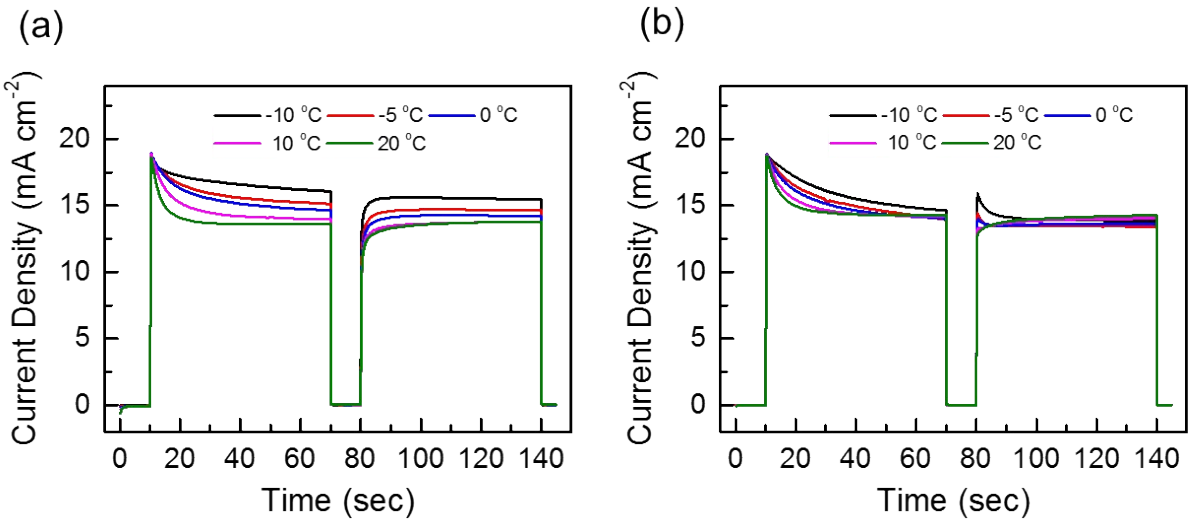

Figure S6. Transient decay of photocurrent density (short circuit condition) against time of PSCs device at different temperature (from -10 °C to 20 °C) under white LED illumination of (a) partially and (b) fully encapsulated device at 0 h storage time.

Table S1. Summary of reported values for activation energy (E_a) in various perovskite-based device configurations.

Device structure	Measurement	E_a (eV)	Contribution
FTO/c-TiO_2/ $MAPbI_{3-x}Cl_x$/spiro-OMeTAD/Ag	Stepwise voltage (dark conditions)	0.31 (forward) 0.23 (reversed)	Migrations of iodide ions/interstitials[4]
FTO/mp-TiO_2/ $MAPbI_3$/spiro-OMeTAD/Au	Stepwise voltage (light conditions)	0.10 – 0.18	V_{MA} facilitate the iodide migration[5]
FTO/mp-TiO_2/ $MAPbI_{3-x}Cl_x$/spiro-OMeTAD/Au	Capacitance-frequency as function of temperature	0.45	Electrode polarization[6]
Glass/$MAPbI_3$/Au	Film conductivity	0.36	MA^+ electromigration[7]
$MAPbI_3$	Theoretical calculation	0.08, 0.46, 0.80	V_I/I_I, V_{MA}, V_{Pb}[8]
		0.32/0.33, 0.57/0.55	V_I/V_I^+, V_{MA}/V_{MA}^+[9]
ITO/PEDOT:PSS/ $MAPbI_3$/PCBM/ C_{60}/Au	Thermally stimulated current	~0.50	Deep trap states[10]
FTO/ mp-TiO_2/ $MAPbI_3$/spiro-OMeTAD/Au	Photoinduced absorption	~0.18	MA ions rotation/ displacement and lattice distortion[11]
FTO/mp-TiO_2/ $MAPbI_3$/spiro-OMeTAD/Au	Temperature dependent photocurrent difference (reversed and forward scan)	0.28	Iodide vacancy migration[12]
ITO/ZnO/MAPbI3/ spiro-OMeTAD/Ag		0.24 (forward) 0.08 (reversed)	Previous work[13]
FTO/c-TiO_2/$MAPbI_{3-x}Cl_x$/spiro-OMeTAD/Ag	Chronoamperometry	~0.60	Iodine migration[14]
ITO/PEDOT:PSS/$MAPbI_3$/$PC_{60}BM$/LiF/Al		0.12	Not mentioned[15]
FTO/mp-TiO_2/$MAPbI_3$/spiro-OMeTAD/Au		0.42	Iodine defect migration[16]
ITO/ZnO/$MAPbI_3$/ spiro-OMeTAD/Ag		**0.23* (forward) 0.19* (reversed) *changes with storage time**	**In this work**

MA = methylammonium, V_I and V_{MA} represents defect vacancies of iodide and methylammonium.

Ca corrosion test

To determine the moisture/O_2 passivation of polyimide (PI) tape as temporary encapsulation, the water vapor transmission rate (WVTR) measurement was carried out by Ca corrosion test. The fabrication process was done by evaporating Ag on top of clean bare glass, followed by Ca with thickness of 100 and 150 nm (deposition rate 0.2 nm/s), respectively, where the size area of Ca was 121 mm^2. It is clearly visible from Fig. S7, the opaque metal color of Ca turns to transparent upon exposure to ambient air. The resistance value was obtained using Keithley 2400 SMU. From the slope of Fig. S7, the PI tape exhibit WVTR value of ~11 $g/m^2/day$ (~60 % RH; 25 ^oC). Meanwhile, the WVTR value of transparent UV cured polyurethane - NOA63 was previously measured around 3 $x10^{-2}$ $g/m^2/day$ (50 % RH; 20^oC) for single polymer/organic passivation layer.[17]

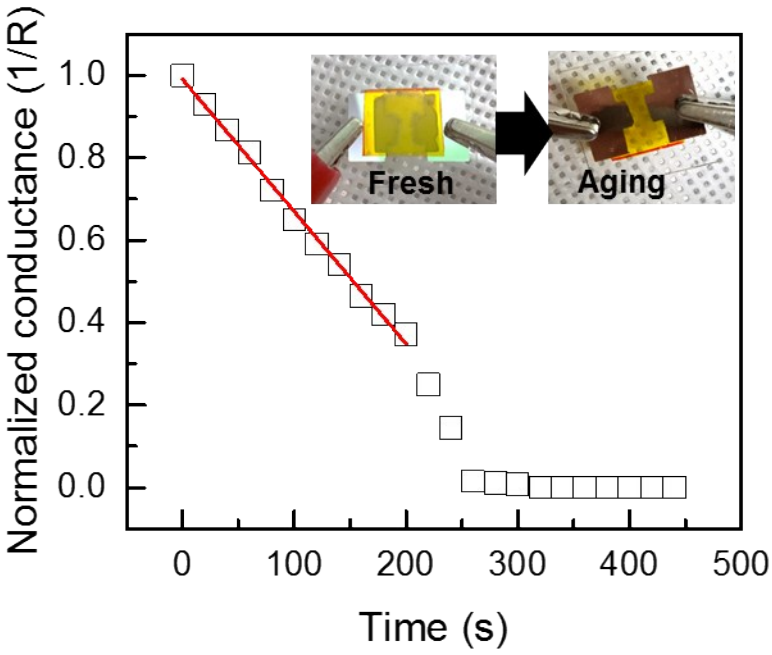

Figure S7. Normalized conductivity against exposure time in ambient air (~60 % RH; 25 ^oC).

Based on the cross-section FESEM images (Fig. S2) after aging at 72 h, it clearly shows the pinhole or void is in accordance with previous reported[18] due to ambient air exposure.

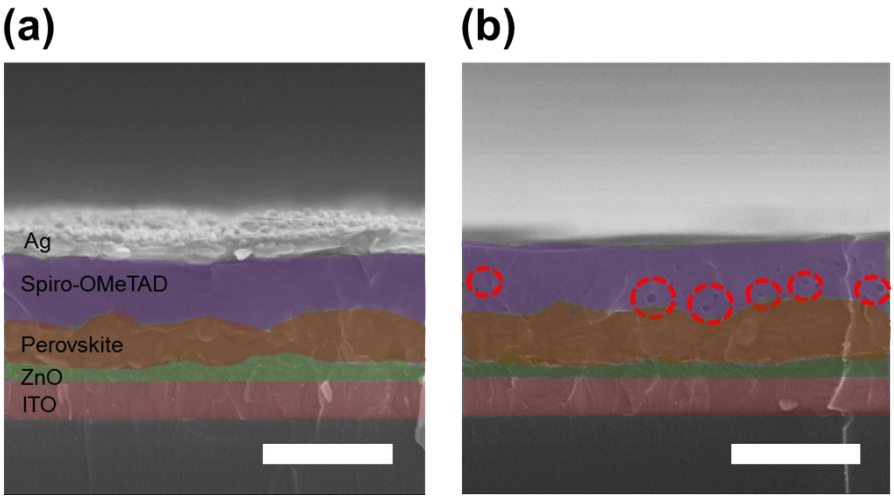

Figure S8. Cross-section FESEM images of (a) Fresh sample and (b) after aging at 72 h in ambient air. The red circle depicts the pinhole distributed within the spiro-OMeTAD layer. Scale bar 500 nm.

References

1. J. Lorrmann, B. H. Badada, O. Inganäs, V. Dyakonov and C. Deibel, *J. Appl. Phys.*, 2010, **108**, 113705.
2. L. K. Ono, P. Schulz, J. J. Endres, G. O. Nikiforov, Y. Kato, A. Kahn and Y. Qi, *J. Phys. Chem. Lett.*, 2014, **5**, 1374-1379.
3. R. S. Sanchez, V. Gonzalez-Pedro, J.-W. Lee, N.-G. Park, Y. S. Kang, I. Mora-Sero and J. Bisquert, *J. Phys. Chem. Lett.*, 2014, **5**, 2357-2363.

4. C. Li, S. Tscheuschner, F. Paulus, P. E. Hopkinson, J. Kießling, A. Köhler, Y. Vaynzof and S. Huettner, *Adv. Mater.*, 2016, **28**, 2446-2454.

5. H. Yu, H. Lu, F. Xie, S. Zhou and N. Zhao, *Adv. Funct. Mater.*, 2016, **26**, 1411-1419.

6. O. Almora, I. Zarazua, E. Mas-Marza, I. Mora-Sero, J. Bisquert and G. Garcia-Belmonte, *J. Phys. Chem. Lett.*, 2015, **6**, 1645-1652.

7. Y. Yuan, J. Chae, Y. Shao, Q. Wang, Z. Xiao, A. Centrone and J. Huang, *Adv. Energy Mater.*, 2015, **5**, 1500615.

8. J. M. Azpiroz, E. Mosconi, J. Bisquert and F. De Angelis, *Energy Environ. Sci.*, 2015, **8**, 2118-2127.

9. J. Haruyama, K. Sodeyama, L. Han and Y. Tateyama, *J. Am. Chem. Soc.*, 2015, **137**, 10048-10051.

10. A. Baumann, S. Väth, P. Rieder, M. C. Heiber, K. Tvingstedt and V. Dyakonov, *J. Phys. Chem. Lett.*, 2015, **6**, 2350-2354.

11. B. Wu, K. Fu, N. Yantara, G. Xing, S. Sun, T. C. Sum and N. Mathews, *Adv. Energy Mater.*, 2015, **5**.

12. S. Meloni, T. Moehl, W. Tress, M. Franckevicius, M. Saliba, Y. H. Lee, P. Gao, M. K. Nazeeruddin, S. M. Zakeeruddin, U. Rothlisberger and M. Graetzel, *Nat. Commun.*, 2016, **7**.

13. R. T. Ginting, E.-S. Jung, M.-K. Jeon, W.-Y. Jin, M. Song and J.-W. Kang, *Nano Energy*, 2016, DOI: http://dx.doi.org/10.1016/j.nanoen.2016.08.016.

14. C. Eames, J. M. Frost, P. R. Barnes, B. C. O'regan, A. Walsh and M. S. Islam, *Nat. Commun.*, 2015, **6**, 7497.

15. D. Bryant, S. Wheeler, B. C. O'Regan, T. Watson, P. R. F. Barnes, D. Worsley and J. Durrant, *J. Phys. Chem. Lett.*, 2015, **6**, 3190-3194.

16. K. Domanski, W. Tress, T. Moehl, M. Saliba, M. K. Nazeeruddin and M. Grätzel, *Adv. Funct. Mater.*, 2015, **25**, 6936-6947.

17. D. Yang, Q. Y. Yong, Y. Duan, P. Chen, C. L. Zang, Y. Xie, D. M. Liu, X. Wang, Y. H. Duan and F. B. Sun, *ECS Solid State Letters*, 2013, **2**, R31-R33.

18. Z. Hawash, L. K. Ono, S. R. Raga, M. V. Lee and Y. Qi, *Chem. Mater.*, 2015, **27**, 562-569.